ISSN 1063-7745, Crystallography Reports, 2020, Vol. 65, No. 2, pp. 223–227. © Pleiades Publishing, Inc., 2020.
Russian Text © The Author(s), 2020, published in Kristallografiya, 2020, Vol. 65, No. 2, pp. 223–228.

STRUCTURE OF INORGANIC COMPOUNDS

Crystal Growth and Temperature Evolution of the Atomic Structure of $Pr_3Ga_5SiO_{14}$ from the Langasite Family

A. P. Dudka[a],* and A. M. Balbashov[b]

[a] *Shubnikov Institute of Crystallography, Federal Scientific Research Centre "Crystallography and Photonics," Russian Academy of Sciences, Moscow, 119333 Russia*

[b] *National Research University MPEI (Moscow Power Engineering Institute), Moscow, 111250 Russia*

* *e-mail: dudka@crys.ras.ru*

Received June 18, 2019; revised October 3, 2019; accepted October 3, 2019

Abstract—$Pr_3Ga_5SiO_{14}$ crystals from the langasite family have been grown by the floating zone melting technique. Their X-ray diffraction analysis is performed at 16 different temperatures in range of 94–293 K. An experiment with ultrahigh resolution at 94 K has yielded the most exact structural model: sp. gr. $P321$, $Z = 1$, $a = 8.07636(4)$ Å, $c = 5.06586(2)$ Å, $R1/wR2 = 1.192/1.185\%$, and $\Delta\rho_{min}/\Delta\rho_{max} = -0.93/+0.79$ e/Å^3 for 3852 unique reflections and 123 refined parameters. The temperature evolution of atomic displacement parameters is estimated based on multitemperature data using the extended Einstein and Debye models. Static components of atomic displacements are selected and the characteristic Einstein and Debye temperatures for structure atoms are determined. No structural anomalies have been found.

DOI: 10.1134/S1063774520020054

INTRODUCTION

Since the time of their discovery, langasite family crystals (structure type $Ca_3Ga_2Ge_4O_{14}$, $a \sim 8.5$ Å, $c \sim 5.1$ Å, sp. gr. $P321$, $Z = 1$ [1, 2]) have been of great interest for researchers due to the variety of their useful physical properties and a large number of possible compositions.

Let us consider the structure of langasite family crystals by an example of the compound $Pr_3Ga_5SiO_{14}$ (PGS). Four cation sites in langasite family crystals A_3BCDO_{14} are in Wyckoff positions in the unit cell: 3*e* (A = Pr, symmetry axis 2; is generally written first in the chemical formula), 1*a* (B = Ga, intersection of symmetry axes 3 and 2), 3*f* (C = Ga, symmetry axis 2), and 2*d* (D = Si, symmetry axis 3). Three independent sites, one special site 2*d* (symmetry axis 3), and two general sites 6*g* are occupied by oxygen atoms (Fig. 1).

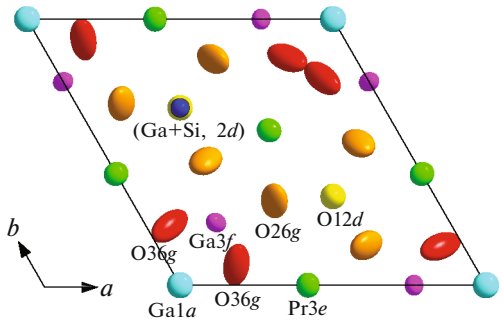

Fig. 1. Projection of the PGS structure on the *ab* plane of unit cell.

Langasite family crystals are used for lasing and as nonlinear optical elements [3]. They are efficient acoustic and piezoelectric materials [4]. In the last years researchers have paid much attention to the compounds of this set that contain magnetic cations [5–7]. In particular, it was found that the langasites containing iron ions in 3*f* sites exhibit antiferromagnetic ordering with a Neel temperature T_N of about 30 K, which is responsible for the multiferroic properties of these compounds [8, 9].

The search of compounds having desired multiferroic characteristics under normal conditions has not yet crowned with success. It was found [10] that an increase in pressure leads to structural transformation and, possibly, magnetic ordering in $Ba_3NdFe_3Si_2O_{14}$ (with Fe in the 3*f* site). NMR measurements on gallium (^{69,71}Ga) and silicon (^{29}Si) nuclei in $Nd_3Ga_5SiO_{14}$ [11], which is a neodymium analog of langasite $La_3Ga_5SiO_{14}$, revealed a large spread in the local environment of neodymium atoms (3*e* site), which leads to disordered exchange coupling. In the last years researchers have intensively investigated [12, 13] the magnetic properties of the praseodymium analog of langasite, PGS, whose structure was described in [4, 14].

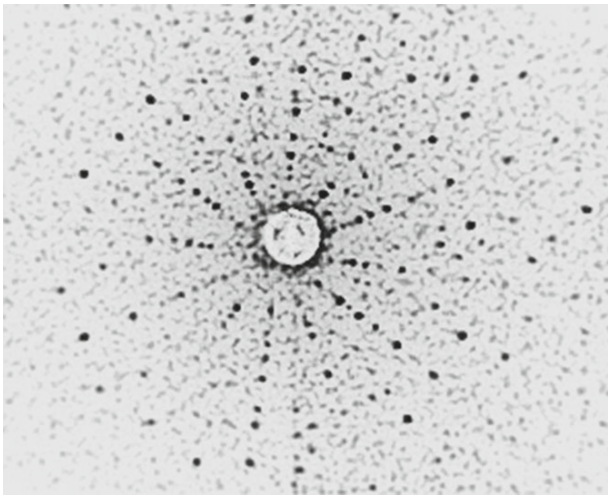

Fig. 2. Laue pattern of PGS crystal.

However, multiferroic properties were not observed in this compound either. One may suggest that, to be fit for practical application, langasite crystals with multiferroic properties should have a more complex structure. It would be of interest to grow a crystal with coexistence of two different magnetic subsystems, composed of atoms occupying the 3*e* site and atoms occupying the 3*f* site.

An example of such a system is ferroborates of rare-earth elements, $RFe_3(BO_3)_4$. Ferroborates are characterized by a number of pronounced multiferroic properties [15, 16]; in particular, they exhibit an elevated (in comparison with langasites) transition temperature to the magnetically ordered state and dependence of the phase-transition temperature on the occupancy of the site with rare-earth element [17].

The most perfect langasites [18] have been grown by the Czochralski method. It is more difficult to grow a compound with iron occupying the 3*f* site; this was done by the floating-zone method in [19, 20]. It is likely that compounds with two magnetic subsystems can be grown more easily using the same technique.

In view of the difficulties related to the growth of these compounds, the first step in this direction was to grow a PGS crystal; this procedure is described below. The diffraction quality of the crystals grown was also estimated, and structural prerequisites of the transition to the magnetically ordered state were sought for. To reveal anomalies, such as implicit phase transitions, partial orderings, and quantum critical points, we used the DebyeFit program for analysis of atomic displacements [21]. Thus, our purpose was to grow PGS single crystals, compare the atomic structure of grown crystals in a wide temperature range, and search for anomalies in the temperature dynamics of structural parameters.

EXPERIMENTAL

Growth of PGS Single Crystal

PGS crystals were grown by the floating zone melting technique on URN-2-ZP growth system in an air medium. The initial agents, Pr_6O_{11}, Ga_2O_3, and SiO_2 (all of special purity grade) were dried at a temperature of 200°C and weighted on a METTLER electronic balance in required amounts in correspondence with the chemical formula. Mixing was performed in a mechanical mixer for 15 min. Preliminary firing of the mixture was performed in air at 1200°C for 6 h. After the grinding the mixture was pressed into rods 10 mm in diameter and 80 mm long (using latex shells) in an isostatic press under a pressure of 1500 atm. The final firing of rods was carried out at a temperature of 1250°C for 6 h. After the firing, cylindrical rods 8 mm in diameter and 70 mm long, with one sharpened end, were prepared by mechanical treatment; these were preforms for growing single crystals by zone melting with light beam heating.

Rods with a cross section of 3×3 mm^2 and 15 mm long, cut from a $La_3Ga_5SiO_{14}$ single crystal, were used as seeds. Cutting was performed after X-ray orientation of crystal in a Photonic Science Laue camera. The crystal growth was carried out in the following modes: linear growth (synchronous motion of the seed and feed rod) with a rate of 2 mm/h, crystal rotation with a rate of 30 rpm, and feed rod rotation with a rate of 1 rpm; the annealing furnace temperature during crystal growth was 1200°C. No additional heat treatments were performed after the growth. The typical sizes of the grown single crystals were as follows: diameter of 4–7 mm and length of 40–50 mm. The quality of grown single crystal was estimated from the Laue pattern structure (Fig. 2). The mosaicity was estimated by checking the coincidence of Laue patterns recorded for different points of the crystal cross section.

Structure of PGS Single Crystal

To increase the diffraction data reliability, the PGS sample was rolled into an ellipsoid with diameters of 0.36–0.39 mm. Sixteen diffraction experiments were performed on an Xcalibur diffractometer with an EOS S2 CCD detector (Rigaku Oxford Diffraction) at nominal temperatures of 86, 90, 100, 110, 120, 130, 140, 150, 160, 170, 180, 190, 200, 230, 260, and 293 K. In correspondence with the calibration performed in [22], the sample temperatures during collection were, respectively, 94, 97, 107, 116, 125, 134, 143, 153, 162, 172, 181, 191, 201, 230, 260, and 293 K. The experiment at 94 K (from here on, the real temperature is indicated) was performed with an ultrahigh resolution to the scattering angle $\theta = 74.5°$; the other measurements were carried out to the angle $\theta = 48.5°$.

The integral intensities were calculated within the CrysAlisPro program [23]. Data processing included the following procedures: consideration of geometric

Table 1. Crystallographic characteristics, experimental details, and results of refinement of the PGS structural model at 94 K

T, K (real)	94
a, c, Å	8.07636(4), 5.06586(2)
V, Å^3	286.165(2)
μ, mm^{-1}	24.27
Diffractometer	Xcalibur EOS S2 CCD
Radiation; λ, Å	MoK_α; 0.71073
Scan mode	ω
Ranges of indices h, k, l	$-21 \le h \le 21$, $-19 \le k \le 20$, $-13 \le l \le 13$
θ_{max}, deg	74.5
Number of measured reflections	29518
Redundancy*	7.44
$\langle\sigma(F^2)/F^2\rangle$	0.0256
$R1_{av}(F^2)/wR2_{av}(F^2)$, %	3.49/6.17
Number of reflections/parameters in refinement	3852/123
$R1(\|F\|)/wR2(\|F\|)$, %	1.193/1.185
S	1.002
$\Delta\rho_{min}/\Delta\rho_{max}$, e/Å^3	−0.93/0.79

1. In each of other 15 experiments, 8350–8380 reflections were measured up to the resolution angle $\theta_{max} = 48.5°$, refinement was finished at $R1(|F|) \sim 1.5$–1.7% for 1700–1730 unique reflections.

2. $R1(|F|) = \Sigma||F_{obs}| - |F_{calc}||/\Sigma|F_{obs}|$; $wR2(|F|) = \sqrt{\{\Sigma w(|F_{obs}| - |F_{calc}|)^2 / \Sigma w(F_{obs})^2\}}$.

* Redundancy is a ratio of the number of measured reflections to the number of unique reflections used in refinement.

features (Lorenz correction) and polarization correction; correction for thermal diffuse scattering [24]; diffractometer calibration [25]; absorption correction [26]; mixed-type extinction correction [27], and refinement of the half-wavelength contribution [28]. All corrections were introduced and structural parameters were refined within the ASTRA program [29]. Fourier syntheses of electron density were constructed using the Jana2006 program [30]. The characteristic Einstein temperatures and static atomic displacements were calculated using the DebyeFit program [21].

All stages of the study (sample preparation, single sample setting throughout the entire experimental series, setting the collection task, and data processing) were aimed at carrying out uniform operations in order to obtain temperature-matched results. The details of data collection and PGS structure refinement are listed in Table 1. The crystallographic data have been deposited with the Cambridge Crystallographic Data Centre (CCDC no. 1967750).

RESULTS AND DISCUSSION

The PGS structure was refined within the sp. gr. $P321$, $Z = 1$, in the anharmonic approximation of atomic displacements. The following refinement criteria were obtained for the experiment at 94 K: $R1/wR2 = 1.192/1.185\%$ and $\Delta\rho_{min}/\Delta\rho_{max} = -0.93/+0.79$ e/Å^3 for 3852 unique reflections and 123 parameters in refinement. The consideration of the anharmonic component of atomic displacements has a high statistical significance: return to the harmonic model increases the R factors to $R1/wR2 = 1.605/1.625\%$ and deteriorates the residual peaks in difference Fourier syntheses to $\Delta\rho_{min}/\Delta\rho_{max} = -2.66/+2.34$ e/Å^3. The rank of atomic displacement tensors (6 322 443 in the notation of [31]: the displacements of atoms Gd(3e), Ga(1a), O1(2d) and O2(6g), and O3(6g) have anharmonic components up to the sixth, third, fourth, and third ranks, respectively) was chosen with the aid of the anharmonic displacement expert [32]. Therefore, the diffraction quality of PGS is comparable with that of iron-containing langasites [19, 20]. The atomic coordinates and atomic displacement parameters for the PGS crystal at a real temperature of 94 K are given in Tables 2 and 3.

The deviations of the temperature dependence of observed atomic displacement parameters $u_{obs} = U_{eq}$ from the theoretical plot are indicative of structural transformation that has already occurred [17] or may occur. The DebyeFit program [21] compares the mul-

Table 2. Atomic coordinates, equivalent thermal parameters U_{eq}, occupancies Q, and ellipsoidalities ε [33] of atomic displacements in the PGS crystal within the anharmonic model at 94 K

Atom	x/a	y/b	z/c	Q	U_{eq}, Å^2	ε
Pr(3e)	0.41811(2)	0	0	1.0	0.00699(3)	0.0187
Ga(1a)	0	0	0	1.0	0.0079(1)	0.0229
Ga(3f)	0.76482(1)	0	1/2	1.0	0.0061(1)	0.0146
(Ga + Si)(2d)	1/3	2/3	0.53513(3)	0.5 + 0.5	0.0051(2)	0.0044
O1(2d)	1/3	2/3	0.1973(6)	1.0	0.0113(8)	0.0137
O2(6g)	0.4665(3)	0.3168(3)	0.3117(4)	1.0	0.0150(5)	0.0413
O3(6g)	0.2222(4)	0.0766(4)	0.7612(4)	1.0	0.0164(2)	0.0594

Table 3. Characteristics of atomic displacements U_{ij} (Å^2) in the PGS crystal within the anharmonic model at 94 K

Atom	U_{11}	U_{22}	U_{33}	U_{12}	U_{13}	U_{23}
Pr(3*e*)	0.00833(4)	0.00915(5)	0.00378(3)	0.00457(3)	0.00026(2)	0.00052(5)
Ga(1*a*)	0.01004(4)	0.0100(3)	0.00370(3)	0.0050(3)	0.0	0.0
Ga(3*f*)	0.00546(2)	0.00635(3)	0.00667(2)	0.0032(4)	−0.001098(9)	−0.0022(3)
(Ga + Si)(2*d*)	0.00545(3)	0.0055(4)	0.00439(3)	0.0027(4)	0.0	0.0
O1(2*d*)	0.0096(6)	0.010(1)	0.0148(8)	0.005(1)	0.0	0.0
O2(6*g*)	0.0119(5)	0.0178(9)	0.0163(5)	0.0083(6)	0.0078(4)	0.0077(4)
O3(6*g*)	0.0165(3)	0.0260(4)	0.0128(2)	0.0152(3)	0.0068(2)	0.0126(2)

titemperature set $u_{obs}(T)$ with the calculated values $u_{calc}(T) = u_{zero} + u_{static} + u_{temp}(T)$, thus separating quantum zero oscillations u_{zero}, static atomic displacements u_{static}, and dynamic thermal oscillations $u_{temp}(T)$. DebyeFit estimates also the Debye temperature T_D and Einstein temperature T_E, which characterize the maximum and average atomic oscillation frequencies, respectively.

The excellent agreement between the values of atomic displacements obtained in this study is confirmed by the low model–experiment reliability factors: $R \sim 1\%$ (Figs. 3, 4; Table 4). The high goodness of fit indicates the absence of structural anomalies. Some deviation from the theoretical dependence is observed for the displacements of oxygen atoms in the range of 130–140 K, but the existing data are insufficient for analysis. An unusual feature is the almost coinciding dynamics of displacements of two oxygen atoms, O2(6*g*) and O3(6*g*), which have different environments. Another extraordinary circumstance is that the Debye temperature for oxygen atoms is fairly low. The maximum oscillation frequencies of anions do not differ much from the average frequencies, $T_D - T_E \approx$ 220 K; therefore, these atoms are not very strongly bound with their far environment. On the whole, the absence of pronounced structural anomalies at 94–293 K is in agreement with the weak magnetism of PGS, which is observed only at ultralow temperatures [12], and with the fact that the main state of PGS is determined to be a spin liquid [13, 14].

CONCLUSIONS

PGS single crystals from the langasite family, containing magnetic ions Pr^{3+} in the 3*e* site, were grown by the floating zone melting technique. The grown crystals have a fairly high diffraction quality, and the prospects of growing a crystal with two magnetic subsystems in atomic sites 3*e* and 3*f* appear to be good. We performed a multitemperature X-ray diffraction study of PGS crystals: 16 datasets were obtained in the temperature range of 94–293 K on an Xcalibur diffractometer with an EOS S2 CCD detector. The main structure characterization was performed based on the ultrahigh-resolution experiment at 94 K: sp. gr. *P*321, $Z = 1$, $a = 8.07636(4)$ Å, $c = 5.06586(2)$ Å, $R1/wR2 =$ 1.192/1.185%, and $\Delta\rho_{min}/\Delta\rho_{max} = -0.93/+0.79$ e/Å^3 for 3852 unique reflections and 123 refined parameters. The multitemperature data were used to deter-

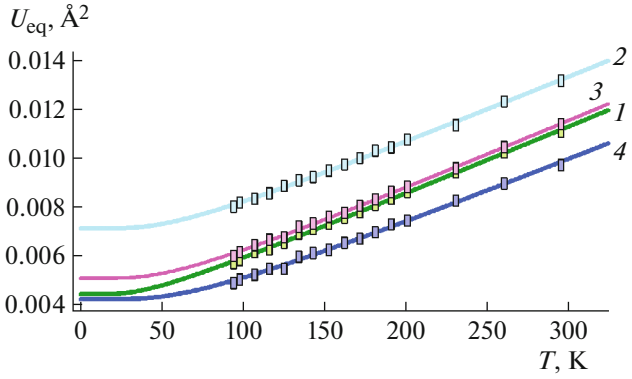

Fig. 3. Equivalent displacement parameters U_{eq} for cations: (*1*) Pr(3*e*), (*2*) Ga(1*a*), (*3*) Ga(3*f*), and (*4*) (Ga + Si, 2*d*); symbols are experimental data and solid lines show the results of fitting experimental parameters U_{eq} using the extended Einstein model.

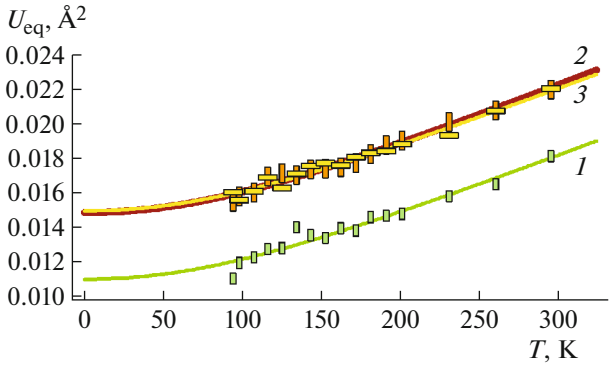

Fig. 4. Equivalent displacement parameters U_{eq} for oxygen atoms : (*1*) O1(2*d*), (*2*) O2(6*g*), and (*3*) O3(6*g*); symbols are experimental data and solid lines show the results of fitting experimental parameters U_{eq} using the extended Debye model.

Table 4. Einstein and Debye temperatures and rms values of static displacements and zero oscillations in PGS crystal

Atom, site	T_E, T_D, K	U_{static}, Å^2	U_{zero}, Å^2	R, %
Pr(3*e*), T_E	111.6(7)	0.00442(5)	0.00154	0.55
Ga(1*a*), T_E	160(2)	0.00707(8)	0.00218	0.48
Ga(3*f*), T_E	157(1)	0.00506(9)	0.00222	0.53
(Ga, Si)(2*d*), T_E	192(2)	0.00425(6)	0.00258	0.87
O1(2*d*), $T_E - T_D$	286(8)–500(13)	0.0111(4)	0.00530	1.97
O2(6*g*), $T_E - T_D$	283(5)–495(8)	0.0149(2)	0.00536	1.23
O3(6*g*), $T_E - T_D$	287(5)–504(9)	0.0150(2)	0.00527	1.18

mine the characteristic Einstein and Debye temperatures for atoms in the structure and select the static components of atomic displacements; this was done for the first time for langasite family crystals. The results obtained show that the structure (especially the cation sublattice) has no anomalies, is consistence with the weak magnetism of PGS [12–14].

FUNDING

This work was supported by the Ministry of Science and Higher Education within the State assignment FSRC "Crystallography and Photonics" RAS. Experimental data was collected using the equipment of the Shared Research Center FSRC "Crystallography and Photonics" RAS and was supported by the Ministry of Science and Higher Education of the Russian Federation (project RFME-FI62119X0035).

REFERENCES

1. E. L. Belokoneva and N. V. Belov, Dokl. Akad. Nauk SSSR, **260** (6), 1363 (1981).
2. E. L. Belokoneva, S. Yu. Stefanovich, Yu. V. Pisarevskii, et al., Russ. J. Inorg. Chem. **45** (11), 1642 (2000).
3. A. A. Kaminsky, B. V. Mill', S. E. Sarkisov, et al., *Physics and Spectroscopy of Laser Crystals* (Nauka, Moscow, 1986) [in Russian], p. 197.
4. B. V. Mill and Yu. V. Pisarevsky, *Proc. IEEE/EIA Int. Frequency Control Symp., Kansas City, Missouru, USA, 2000,* p. 133.
5. V. Yu. Ivanov, A. A. Mukhin, A. S. Prokorov, and B. V. Mill, Solid State Phenom. **152–153**, 299 (2009).
6. H. D. Zhou, L. L. Lumata, P. L. Kuhns, et al., Chem. Mater. **21**, 156 (2009).
7. K. Marty, P. Bordet, V. Simonet, et al., Phys. Rev. B **81**, 054416 (2010).
8. I. S. Lyubutin, P. G. Naumov, B. V. Mill', et al., Phys. Rev. B **84**, 214425 (2011).
9. S. A. Pikin and I. S. Lyubutin, Phys. Rev. B **86**, 4414 (2012).
10. A. G. Ivanova, I. A. Troyan, S. S. Starchikov, et al., *Abstracts 56th EHPRG Meeting, Aveiro, Portugal, September 2–7, 2018,* p. 114.
11. A. Zorko, F. Bert, P. Bordet, et al., J. Phys.: Conf. Ser. **145**, 012006 (2009).
12. H. D. Zhou, C. R. Wiebe, Y. J. Yo, et al. arXiv:cond-mat/0808.2819
13. A. Zorko, F. Bert, P. Mendels, et al. arXiv:cond-mat/0912.4648
14. L. L. Lumata, T. Besara, P. L. Kuh, et al., Phys. Rev. B **81**, 224416 (2010).
15. A. N. Vasiliev and E. A. Popova, Low Temp. Phys. **32**, 735 (2006).
16. M. Kadomtseva, Yu. F. Popov, G. P. Vorob'ev, et al., Low Temp. Phys. **36**, 511 (2010).
17. E. S. Smirnova, O. A. Alekseeva, A. P. Dudka, et al., Acta Crystallogr. B **74**, 226 (2018).
18. A. P. Dudka, Crystallogr. Rep. **61** (2), 187 (2016).
19. A. R. Dudka, A. V. Balbashov, and I. S. Lyubutin, Cryst. Growth Des. **16**, 4943 (2016).
20. A. P. Dudka, A. M. Balbashov, and I. S. Lyubutin, Crystallogr. Rep. **61** (1), 24 (2016).
21. A. P. Dudka, N. B. Bolotina, and O. N. Khrykina, J. Appl. Crystallogr. **52**, 690 (2019).
22. A. P. Dudka, I. A. Verin, and E. S. Smirnova, Crystallogr. Rep. **61** (4), 692 (2016).
23. Rigaku Oxford Diffraction, *CrysAlisPro Software System, version 1.171.39.46* (Rigaku Corporation, Oxford, UK, 2018).
24. A. P. Dudka, M. Kh. Rabadanov, and A. A. Loshmanov, Kristallografiya **34** (4), 818 (1989).
25. A. Dudka, J. Appl. Crystallogr. **43** (6), 1440 (2010).
26. A. P. Dudka, Crystallogr. Rep. **50** (6), 1068 (2005).
27. P. J. Becker and P. Coppens, Acta Crystallogr. A **30**, 129 (1974).
28. A. Dudka, J. Appl. Crystallogr. **43** (1), 27 (2010).
29. A. Dudka, J. Appl. Crystallogr. **40** (3), 602 (2007).
30. V. Petricek, M. Dusek, and L. Palatinus, Z. Kristallogr. **229** (5), 345 (2014).
31. A. P. Dudka and B. V. Mill', Crystallogr. Rep. **56** (3), 443 (2011).
32. A. P. Dudka, Crystallogr. Rep. **53** (2), 351 (2008).
33. A. P. Dudka and B. V. Mill', Crystallogr. Rep. **59** (5), 689 (2014).

Translated by Yu. Sin'kov